

## Original Article

**Cite this article:** Chetvertkov MA, Vassiliev ON, Yang J, Wang HC, Liu AY, Liao Z, and Mohan R. (2021) Impact of intra-fractional motion on dose distributions in lung IMRT. *Journal of Radiotherapy in Practice* **20**: 12–16. doi: [10.1017/S1460396919000967](https://doi.org/10.1017/S1460396919000967)

Received: 30 October 2019  
Revised: 26 November 2019  
Accepted: 30 November 2019  
First published online: 9 January 2020

### Key words:


dose accuracy; intra-fractional motion; lung IMRT; PTV coverage

### Author for correspondence:

Oleg N. Vassiliev, Department of Radiation Physics, The University of Texas MD Anderson Cancer Center, 1400 Pressler St., Houston, TX 77030, USA. Tel: 713-745-7995; Fax: 713-563-6949; Email: [onvassil@mdanderson.org](mailto:onvassil@mdanderson.org)

\*Present address: Department of Radiation Oncology, Allegheny General Hospital, 320 E North Ave, Pittsburgh, PA 15212, USA

# Impact of intra-fractional motion on dose distributions in lung IMRT

Mikhail A. Chetvertkov<sup>1,a</sup>, Oleg N. Vassiliev<sup>1</sup> , Jinzhong Yang<sup>1</sup>, He C. Wang<sup>1</sup>, Amy Y. Liu<sup>1</sup>, Zhongxing Liao<sup>2</sup> and Radhe Mohan<sup>1</sup>

<sup>1</sup>Department of Radiation Physics, The University of Texas MD Anderson Cancer Center, 1400 Pressler St., Houston, TX 77030, USA and <sup>2</sup>Division of Radiation Oncology, The University of Texas MD Anderson Cancer Center, 1400 Pressler St, Houston, TX 77030, USA

## Abstract

**Aim:** To investigate the impact of intra-fractional motion on dose distribution in patients treated with intensity-modulated radiotherapy (IMRT) for lung cancer.

**Materials and methods:** Twenty patients who had undergone IMRT for non-small cell lung cancer were selected for this retrospective study. For each patient, a four-dimensional computed tomography (CT) image set was acquired and clinical treatment plans were developed using the average CT. Dose distributions were then recalculated for each of the 10 phases of respiratory cycle and combined using deformable image registration to produce cumulative dose distributions that were compared with the clinical treatment plans.

**Results:** Intra-fractional motion reduced planning target volume (PTV) coverage in all patients. The median reduction of PTV covered by the prescription isodose was 3.4%;  $D_{98}$  was reduced by 3.1 Gy. Changes in the mean lung dose were within  $\pm 0.7$  Gy.  $V_{20}$  for the lung increased in most patients; the median increase was 1.6%. The dose to the spinal cord was unaffected by intra-fractional motion. The dose to the heart was slightly reduced in most patients. The median reduction in the mean heart dose was 0.22 Gy, and  $V_{30}$  was reduced by 2.5%. The maximum dose to the oesophagus was also reduced in most patients, by 0.74 Gy, whereas  $V_{50}$  did not change significantly. The median number of points in which dose differences exceeded 3%/3 mm was 6.2%.

**Findings:** Intra-fractional anatomical changes reduce PTV coverage compared to the coverage predicted by clinical treatment planning systems that use the average CT for dose calculation. Doses to organs at risk were mostly over-predicted.

## Introduction

The primary motivation for this study was to determine the need to account for respiratory motion when estimating intensity-modulated radiotherapy (IMRT) dose distributions in correlative studies of dosimetric indices and patient outcomes.

Intra-fractional changes in patient anatomy, most importantly those caused by respiration, introduce uncertainties in delivered dose distributions in lung cancer patients. Current treatment planning techniques determine the extent of tumour motion by four-dimensional computed tomography (4DCT), and plans are designed to ensure tumour coverage at all phases of the respiratory cycle. However, these methods do not explicitly account for all anatomical changes, most importantly those in organs in the beam path and near the tumour. For these reasons, differences between planned and delivered dose distributions may be significant, potentially resulting in suboptimal treatment.

Several recent studies have investigated the dosimetric impact of respiratory motion on lung cancer treatment<sup>1–8</sup>. The approach in these studies was based on the use of 4DCT image sets. Dose distributions were first calculated separately for each of the three-dimensional (3D) CT images in the 4DCT dataset. The 3D dose distributions were then combined (accumulated) using deformable image registration techniques to obtain the distribution of the total dose delivered. Flampouri et al.<sup>1</sup> performed such calculations for a cohort of six lung cancer patients treated with IMRT, using four planning techniques for each patient. They reported underdosage of the clinical target volume (CTV) in the two patients with the largest extent of tumour motion in the cohort. The largest underdosage, expressed as the equivalent uniform dose, was 33 Gy. Conventional 3D treatment planning was performed on a free-breathing CT image. The study reported significant free-breathing image artefacts that contributed to the differences between the conventional and 4DCT doses.

In contrast to Flampouri et al.<sup>1</sup>, Guckenberger et al.<sup>2</sup>, who evaluated 3D conformal plans in a cohort of seven patients, used the end-exhalation CT as the reference image for the reference 3D plan because tumour motion and image artefacts are expected to be minimal with this

choice. Dose distributions for each phase of the respiratory cycle were calculated using the respective CT image and the collapsed cone convolution superposition algorithm. All secondary CT images were registered to the reference image using a surface model-based deformable registration algorithm. The deformation maps were applied to map dose distributions to the reference image and thereby find the dose accumulated over the entire cycle. The 3D reference doses to the gross tumour volume (GTV) and internal target volume (ITV) were good approximations of the 4D dose calculations, and the 3D and 4D doses to the ipsilateral lung (that included the GTV) were similar.

Rosu et al.<sup>3</sup> studied a larger cohort (15 patients) and used simplified planning techniques, anterior-posterior/posterior-anterior beams and 3D conformal plans. A further simplification was that instead of the full 4DCT image set, the study used only exhalation and inhalation CT images. The authors reported that changes in the equivalent uniform dose for the CTV were minimal. Some differences between the 3D and 4DCT doses were reported for the normal lung tissue. In the worst case, a 6-Gy decrease in the prescription dose was required in an iso-normal tissue complication probability dose escalation protocol to compensate for the difference.

In a study by Admiraal et al.<sup>4</sup> of 10 stage I lung cancer patients, the focus was on the dose to the CTV. The study found that breathing motion did not cause significant differences in CTV coverage, even when the margin from the ITV to planning target volume (PTV) was set to 0. Roland et al.<sup>5</sup> studied a cohort of six patients with an extent of tumour motion of 2–10 mm. The differences between the 3D and 4DCT dose distributions were small. The study concluded that patient population exists in which '4D planning does not provide any additional benefits beyond that afforded by 3D planning'.

Huang et al.<sup>6</sup> considered only two patient cases. They reported that for a smaller tumour (GTV of 12.5 cm<sup>3</sup>) with a motion extent of 1.5 cm, the 4DCT dose calculation revealed reduced tumour coverage. This was not the case for a larger tumour (159.1 cm<sup>3</sup>) with a motion range of 1 cm. Chan et al.<sup>7</sup> investigated dose distributions in real-time tumour tracking stereotactic body radiation therapy with Cyberknife (Accuray, Inc., Sunnyvale, CA). When comparing 4D and 3D dose calculations in 25 patients, the authors found only minimal differences for normal tissues. Only moderate differences were seen for the GTV. The generalised equivalent uniform dose was reduced by a mean of 2.8 Gy, and the corresponding reduction in tumour control probability was 1.6%.

Li et al.<sup>8</sup> proposed an analytical technique for quantifying motion-induced dose uncertainties that consider a multitude of factors, including the treatment delivery dose rate and the duration of the respiratory cycle. They applied this technique retrospectively to 10 lung cancer IMRT patients and found that the mean deviation of the planned dose from the 4DCT dose in the PTV was less than 2.5% and the maximum point dose variation in the PTV was <6.2%.

In this retrospective study, we investigated the differences between dose distributions that were calculated for a static reference CT image set and dose distributions that were calculated to account for intra-fractional motion using individual 3D phases of the 4DCT image sets. The study cohort was composed of 20 patients who had been treated with IMRT for advanced lung cancer. It included patients with a wide range of tumour sizes, locations and extents of motion. Similar to the previous studies we report on tumour coverage. We extend prior reports by examining doses to normal tissues surrounding the tumour and by

**Table 1.** Patient cohort characteristics

Characteristic	Value
Sex, n (%)	
Male	11 (55)
Female	9 (45)
Disease stage, n (%)	
IA	1 (5)
IIA	2 (10)
IIB	3 (15)
IIIA	11 (55)
IIIB	3 (15)
Tumour histologic type, n (%)	
Adenocarcinoma	11 (55)
Squamous cell carcinoma	6 (30)
Non-small cell lung cancer	3 (15)
Prescription dose (Gy), n (%)	
60	1 (5)
66	5 (25)
70	1 (5)
74	13 (65)
Tumour characteristics, median (range)	
Gross tumour volume, cm <sup>3</sup>	69.0 (10.2–269.7)
Diameter of gross tumour volume, cm	5.1 (3.0–8.0)
Planning target volume, cm <sup>3</sup>	380.8 (155.2–890.8)
Diameter of planning target volume, cm	9.0 (6.7–11.9)
Tumour motion, cm	0.6 (0.1–2.2)
Age, median (range)	64 (48–68)

performing detailed, point-by-point comparisons of dose distributions throughout the entire treated volume.

## Methods and Materials

### Patient cohort

Twenty patients who had undergone IMRT for early-stage and locally advanced non-small cell lung cancer were selected for this study. The patients were selected so that the cohort included a representative range of tumour sizes, motions and locations. The patients had been treated in 2010–2014. The cohort's characteristics are summarised in Table 1. The study was conducted under a protocol approved by the Institutional Review Board.

### Treatment planning

Four-dimensional CT image sets for each patient were acquired on a GE LightSpeed 16-slice scanner (GE Medical Systems, Waukesha, WI). Four-dimensional image reconstruction was performed using Advantage 4D software (GE Medical Systems, Waukesha, WI), and respiratory traces were recorded with the real-time position management system (Varian Medical Systems, Palo Alto, CA). The breathing cycle was divided into

**Table 2.** Summary of dosimetric differences between 4DCT and average CT calculations

Dosimetric index	Median	Interquartile range	Index improved, patients (%)	p-Value
<b>iGTV</b>				
$V_x(4DCT)/V_x(Av)$	1.000	0.999, 1.000	1 (5)	0.3
<b>CTV</b>				
$V_x(4DCT)/V_x(Av)$	0.997	0.989, 1.000	5 (25)	0.02
<b>PTV</b>				
$V_x(4DCT)/V_x(Av)$	0.966	0.926, 0.989	0 (0)	<0.001
$D_{98}(4DCT) - D_{98}(Av)$ , cGy	-310	-610, -120	0 (0)	<0.001
<b>Total lung</b>				
$D_{mean}(4DCT) - D_{mean}(Av)$ , cGy	4	-20, 28	8 (40)	0.6
$V_{20}(4DCT)/V_{20}(Av)$	1.016	0.992, 1.032	6 (30)	0.07
<b>Spinal cord</b>				
$D_{max}(4DCT) - D_{max}(Av)$ , cGy	-10	-36, 23	14 (70)	0.3
<b>Oesophagus</b>				
$D_{max}(4DCT) - D_{max}(Av)$ , cGy	-74	-148, -8	15 (75)	0.002
$V_{50}(4DCT)/V_{50}(Av)$	1.00	0.978, 1.014	9 (45)	0.8
<b>Heart</b>				
$D_{mean}(4DCT) - D_{mean}(Av)$ , cGy	-22	-52, -2	19 (95)	<0.001
$V_{30}(4DCT)/V_{30}(Av)$	0.975	0.982, 1.043	14 (70)	0.005

Abbreviations: 4DCT, four-dimensional computed tomography; iGTV, gross tumour volume motion; CTV, clinical target volume; PTV, planning target volume.

10 phases; therefore, each 4DCT dataset was composed of 10 3D images. In addition, for each patient, a maximum intensity projection (MIP) and an average CT images were generated. We determined the envelope of GTV motion (iGTV) on all 10 phases of the 4DCT by contouring the GTV on the maximum MIP and then reviewing it across all 10 phases and editing it as necessary. The ITV was then generated by expanding the iGTV by 8 mm, and the PTV was created by expanding the ITV by 5 mm.

IMRT treatment planning was performed on the average CT image set using the Pinnacle treatment planning system (Philips Radiation Oncology Systems, Fitchburg, WI). The prescription doses ranged from 66 to 74 Gy, delivered in 200 or 220 cGy per fraction. The number of beams was 7–11. Most beams, except 1 or 2 beams per patient, were co-planar. The most common prescription was 74 Gy in 37 fractions, planned with 11 beams. Prescriptions specified the volume to be covered by the prescription dose. This volume ranged from 95 to 97.5% of the PTV, or in two cases, the GTV.

#### Four-dimensional dose calculation

For each patient, the dose distribution was calculated for each of the 10 CT images representing 10 phases of the respiratory cycle. The calculations were performed in Pinnacle using the original treatment plan with the prescription set to deliver the same number of monitor units and the same collapsed cone convolution algorithm with the same setting as in the original treatment plan. Ten calculated doses (for the 10 phases) and the respective 10 CT images were imported into an in-house deformable image registration software tool, which is based on the dual-force

Demons algorithm<sup>9,10</sup>. The CT image for each given phase was registered to the image for the end-of-exhalation phase (T50). The resultant deformation vector fields were then used to map the corresponding dose at each phase to the T50 image. The individual deformed doses were summed together to generate the dose accumulated over the respiratory cycle. To compare the accumulated dose with the planned dose distributions, we mapped the former on the planning CT.

#### Dose comparison

Dose distributions were compared using the plan evaluation tools of the Pinnacle treatment planning system. For a detailed analysis of dose differences, MATLAB (Version 2014b, MathWorks, Natick, MI) code was written. The code compares doses point by point, calculates the distance to agreement in 3D and a 3D gamma index and outputs several metrics that characterise the differences between two dose distributions.

#### Statistical analysis

For the analysis of differences between planned and 4DCT doses, we used the Wilcoxon signed-rank test, a non-parametric statistical hypotheses test.

## Results and Discussion

#### Tumour coverage

A summary of dose comparisons for the PTV, CTV and iGTV is given in Table 2. Intra-fractional motion reduced PTV coverage

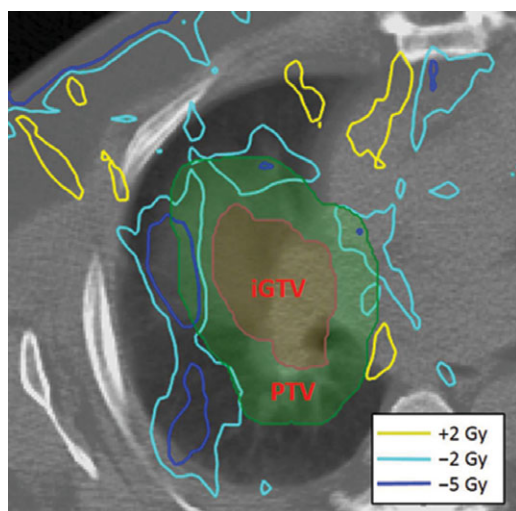


**Figure 1.** An example of differences between the 4D dose calculation and the dose calculated on average computed tomography (planned dose):  $\Delta D = D(4D) - D(Av)$ . Dark blue, aqua and yellow lines show  $\Delta D = -5$ ,  $-2$  and  $+2$  Gy, respectively. Abbreviations: PTV, planning target volume; iGTV, gross tumour volume motion.

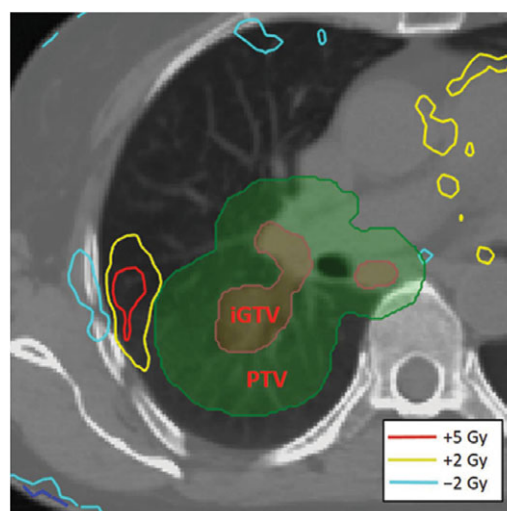


**Figure 3.** An example of differences between the 4D dose calculation and the dose calculated on average computed tomography (planned dose):  $\Delta D = D(4D) - D(Av)$ . Aqua, yellow and red lines show  $\Delta D = -2$ ,  $+2$  and  $+5$  Gy, respectively. Abbreviations: PTV, planning target volume; iGTV, gross tumour volume motion.

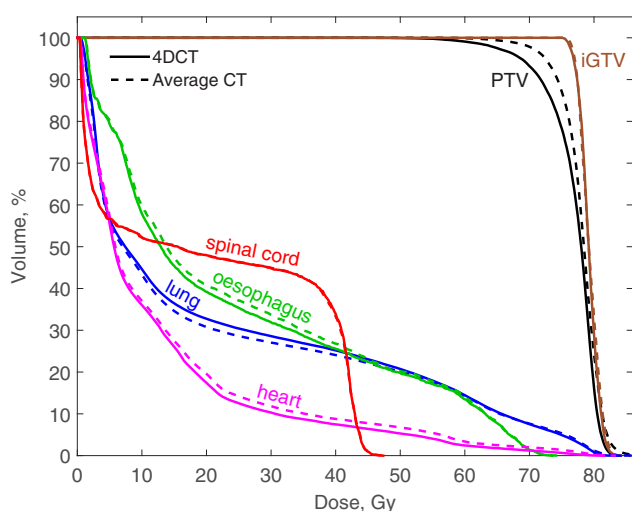


**Figure 2.** The dose-volume histogram for a case in which the difference in PTV coverage between 4DCT and the average CT dose was considerable. Shown is the same patient as in Figure 1. Abbreviations: PTV, planning target volume; 4DCT, four-dimensional computed tomography; iGTV, gross tumour volume motion.

in all patients compared to planned dose distributions that had been calculated using the average CT. The median reduction of the PTV covered by the prescription isodose was 3.4%, and the interquartile range (IQR) was (1.1, 7.4%). Similarly, the  $D_{98}$  for the PTV was also reduced in all patients. The median reduction was 3.1 Gy, and the IQR was (1.2, 6.1 Gy). While the median reduction in both cases was modest, reduction in PTV coverage was seen in all patients, and in some patients, the calculated underdosage was considerable. It is therefore important to identify, prior to treatment, patients who are at a higher risk of underdosage and take corrective actions to ensure uncompromised PTV coverage. Risk can be initially assessed by reviewing intra-fractional anatomical changes on 4DCT image sets, for example, by comparing images obtained at inspiration and expiration. We were unable to identify a simple characteristic that was predictive of PTV underdosage: tumour size, tumour or

diaphragm motion and location did not correlate with the metrics of PTV underdosage.

Current treatment planning techniques do account for the extent of tumour motion. Our data suggest that the movement of tissues surrounding the tumour and those in the beam path should also be considered. For a more definitive and quantitative risk evaluation, a full 4DCT dose calculation, or a calculation on a reduced 4D dataset (i.e. using fewer than the usual 10 respiratory phases), may be necessary.

Figure 1 illustrates the reduction in PTV coverage in a case in which the differences between 4DCT and average CT dose distributions were particularly large. The figure shows  $\Delta D = D(4D) - D(Av)$ . Aqua and dark blue lines show  $\Delta D = -2$  and  $-5$  Gy, respectively. Yellow lines show  $\Delta D = +2$  Gy. Calculations using the average CT over-predicted the dose by 5 Gy or more in some peripheral regions of the PTV. The dose-volume histogram for the same patient is shown in Figure 2. In this case, the  $V_{95}$  for the PTV was lower by 3.7 Gy when intra-fractional motion anatomical changes were accounted for. On the other hand, the iGTV coverage remained the same as in the planned dose distribution. Overall, dose coverage of the iGTV was not significantly affected by respiratory motion. On the other hand, the CTV covered by the prescription isodose was reduced in most patients; however, the reduction was small, on the order of 1%.

### Doses to normal tissues

A summary of dose comparisons for the lung, oesophagus, spinal cord and heart is given in Table 2. Respiratory motion had little effect on the mean lung dose. The differences in mean lung doses between 4DCT and the mean CT were within  $\pm 0.7$  Gy. However, in most patients, the  $V_{20}$  for the lung was higher when the dose was calculated using 4DCT images. The median increase in the  $V_{20}$  was small, only 1.6%. In the worst case, the  $V_{20}$  increased by 7.9% but remained well within the tolerance limits. An example of an increased lung dose is shown in Figure 3. The dose to the spinal cord was largely unaffected by the respiratory motion (see, e.g., the dose-volume histogram in Figure 2). Differences in the maximum dose to the cord between 4DCT and planned doses

were within  $\pm 0.9$  Gy. The maximum dose to the oesophagus was reduced in most (75%) patients. The median reduction was 0.74 Gy. In the worst case, the maximum dose increased by 0.5 Gy. Changes in  $V_{50}$  for the oesophagus ranged from  $-7\%$  to  $+6\%$ , and the median change was 0.00. Doses to the heart, calculated using 4DCT images, were lower in most patients than were the planned doses. Dose reductions in the mean heart dose and the  $V_{30}$  were both significant. All dosimetric indices for the lung that were recalculated using 4DCT images remained within the standard tolerance limits in all patients.

### Point-by-point dose comparison

We performed point-by-point dose comparisons of dose distributions that were planned versus those that were calculated using 4DCT images. We found that the median number of dose points where the dose difference exceeded 3% and the distance to agreement exceeded 3 mm was 6.2%; the corresponding IQR was (1.8, 7.8%). In these calculations, the percentage of dose difference was expressed in terms of the local dose. For this reason, this analysis was performed only in the volume where the dose exceeded 10% of the maximum dose.

As can be seen in Figures 2 and 3, differences between the planned and 4DCT doses exceeding 5 Gy were not uncommon. The median volume where the 4DCT dose was lower than the planned dose by more than 5 Gy was 138 cm<sup>3</sup> (IQR 65, 251 cm<sup>3</sup>). The median volume in which the 4DCT dose was higher by more than 5 Gy was 229 cm<sup>3</sup> (IQR 160, 331 cm<sup>3</sup>). The average dimensions of the volumes in which patients received doses more than 5 Gy higher than planned were a few cm and in the normal lung (five patients, shown for example by the red contour in Figure 3), mediastinum (two patients) and chest wall (one patient). However, in no cases did the dose-volume metrics exceed the standard tolerance limits.

### Impact on clinical practice

This study produced data on the magnitude and patterns of dose variations caused by intra-fractional motion. This information is important for the always ongoing review of treatment outcomes. Our results, for example, bring attention to the reduction of target coverage by the prescription isodose. This reduction should be considered in review of local recurrence cases as a potential risk factor.

### Limitations of the study

In addition to respiratory motion, the actual doses delivered to patients are affected by daily setup uncertainties and inter-fractional anatomical changes. We did not consider these two factors, as our focus has been on quantifying and understanding the impact of intra-fractional changes. Analysis of the other sources of uncertainties in delivered doses is no less important, but is probably more appropriate for a separate study.

### Conclusions

The main impact of intra-fractional anatomical changes was a reduction in PTV coverage compared to that predicted by the

treatment planning system in which dose calculations were performed on the average CT image. This reduction was caused not only by tumour motion but also by changes in nearby tissues in the beam path, such as the rib cage. While the PTV is designed to account for all geometric uncertainties, it remains possible that inter-fractional positioning uncertainties, in addition to respiratory motion, may exceed margins in specific patients and may lead to underdosing in the CTV and even the GTV.

Developing a practical method for evaluating the dosimetric impact of intra-fractional motion prior to treatment would help mitigate such risks. In this study, we did not find any cases in which treatment planning using the average CT significantly underestimated doses to the heart, spinal cord and oesophagus. In the planned dose distribution, the  $V_{20}$  for the lung was underestimated in most patients. This underestimation, however, was not statistically significant in this study cohort.

**Acknowledgements.** This study was supported in part by the National Institutes of Health grant U19 CA-21239.

**Financial Support.** Grant support: NIH grant U19 CA-21239.

**Conflicts of Interest.** None.

### References

1. Flampouri S, Jiang SB, Sharp GC et al. Estimation of the delivered patient dose in lung IMRT treatment based on deformable registration of 4D-CT data and Monte Carlo simulations. *Phys Med Biol* 2006; 51: 2763–2779.
2. Guckenberger M, Wilbert J, Krieger T et al. Four-dimensional treatment planning for stereotactic body radiotherapy. *Int J Radiat Oncol Biol Phys* 2007; 69: 276–285.
3. Rosu M, Chetty IJ, Tatro DS, Ten Haken RK. The impact of breathing motion versus heterogeneity effects in lung cancer treatment planning. *Med Phys* 2007; 34: 1462–1473.
4. Admiraal MA, Schuring D, Hurkmans CW. Dose calculations accounting for breathing motion in stereotactic lung radiotherapy based on 4D-CT and the internal target volume. *Radiother Oncol* 2008; 86: 55–60.
5. Roland T, Mavroidis P, Gutierrez A, Goytia V, Papanikolaou N. A radiobiological analysis of the effect of 3D versus 4D image-based planning in lung cancer radiotherapy. *Phys Med Biol* 2009; 54: 5509–5523.
6. Huang TC, Liang JA, Dilling T, Wu TH, Zhang G. Four-dimensional dosimetry validation and study in lung radiotherapy using deformable image registration and Monte Carlo techniques. *Radiat Oncol* 2010; 5: 45
7. Chan MKH, Kwong DLW, Ng SCY, Tam EK, Tong AS. Investigation of four-dimensional (4D) Monte Carlo dose calculation in real-time tumor tracking stereotactic body radiotherapy for lung cancers. *Med Phys* 2012; 39: 79–87
8. Li H, Park P, Liu W et al. Patient-specific quantification of respiratory motion-induced dose uncertainty for step-and-shoot IMRT of lung cancer. *Med Phys* 2013; 40: 121712
9. Wang H, Dong L, Lii MF et al. Implementation and validation of a three-dimensional deformable registration algorithm for targeted prostate cancer radiotherapy. *Int J Radiat Oncol Biol Phys* 2005; 61: 725–735
10. Wang H, Garden AS, Zhang L et al. Performance evaluation of automatic anatomy segmentation algorithm on repeat or four-dimensional computed tomography images using deformable image registration method. *Int J Radiat Oncol Biol Phys* 2008; 72: 210–219